Author/s:
Martelli, F;Ravenscroft, TA;Hutchison, W;Batterham, P

Title:
Tissue-specific transcriptome analyses in Drosophila provide novel insights into the mode of action of the insecticide spinosad and the function of its target, nAChRα6

Date:
2023-10

Citation:
Martelli, F., Ravenscroft, T. A., Hutchison, W. & Batterham, P. (2023). Tissue-specific transcriptome analyses in Drosophila provide novel insights into the mode of action of the insecticide spinosad and the function of its target, nAChRα6. Pest Management Science, 79 (10), pp.3913-3925. https://doi.org/10.1002/ps.7585.

Persistent Link:
https://hdl.handle.net/11343/354183

Research Article

Received: 4 April 2023 Revised: 24 May 2023 Accepted article published: 29 May 2023 Published online in Wiley Online Library:

(wileyonlinelibrary.com) DOI 10.1002/ps.7585

Tissue-specific transcriptome analyses in *Drosophila* provide novel insights into the mode of action of the insecticide spinosad and the function of its target, *nAChRα6*

Felipe Martelli,[a*] Thomas A. Ravenscroft,[b] William Hutchison[a] and Philip Batterham[a]

Abstract

BACKGROUND: The insecticides spinosad and imidacloprid are neurotoxins with distinct modes of action. Both target nicotinic acetylcholine receptors (nAChRs), albeit different subunits. Spinosad is an allosteric modulator, that upon binding initiates endocytosis of its target, nAChRα6. Imidacloprid binding triggers excessive neuronal ion influx. Despite these differences, low-dose effects converge downstream in the precipitation of oxidative stress and neurodegeneration.

RESULTS: Using RNA-sequencing, we compared the transcriptional signatures of spinosad and imidacloprid, at low-dose exposures. Both insecticides cause up-regulation of glutathione S-transferase and cytochrome P450 genes in the brain and down-regulation in the fat body, whereas reduced expression of immune-related genes is observed in both tissues. Spinosad shows unique impacts on genes involved in lysosomal function, protein folding, and reproduction. Co-expression analyses revealed little to no correlation between genes affected by spinosad and *nAChRα6* expressing neurons, but a positive correlation with glial cell markers. We also detected and experimentally confirmed *nAChRα6* expression in fat body cells and male germline cells. This led us to uncover lysosomal dysfunction in the fat body following spinosad exposure, and a fitness cost in spinosad-resistant (*nAChRα6* null) males – oxidative stress in testes, and reduced fertility.

CONCLUSION: Spinosad and imidacloprid share transcriptional perturbations in immunity-, energy homeostasis-, and oxidative stress-related genes. Low doses of other neurotoxic insecticides should be investigated for similar impacts. While target-site spinosad resistance mutation has evolved in the field, this may have a fitness cost. Our findings demonstrate the power of tissue-specific transcriptomics approach and the use of single-cell transcriptome data.

Supporting information may be found in the online version of this article.

Keywords: brain; fat body; testes; co-expression analysis; fitness cost; lysosome

1 INTRODUCTION

The extensive use of insecticides is the most common way of controlling agricultural pests and insects that vector pathogens.[1–3] Crop yields are increased by 6–79% as a result of insecticide use.[3,4] With demands for increased food production to match the growing global population, insecticides have an important role. However, there is limited understanding of how low insecticide doses that contaminate environments affect non-pest insects. This knowledge is important to understand the role of insecticides on insect population declines.[5]

Two recent studies conducted in parallel on the effects of low-dose impacts of the neurotoxic insecticides imidacloprid[6] and spinosad[7] in *Drosophila melanogaster*, detailed their distinct mechanisms of action that yielded similar cascades of damage. Both insecticides target nicotinic acetylcholine receptors (nAChRs) in the insect central nervous system (CNS). The nAChRs are ligand-gated cation channels, conserved among insects that, once activated, lead to calcium ion (Ca^{2+}), sodium ion (Na^{+}), or potassium ion (K^{+}) flux into neurons, regulating a range of neuromotor and behavioural responses.[8] Imidacloprid targets subunits

* *Correspondence to: F Martelli, School of BioSciences, The University of Melbourne, Melbourne, VIC 3052, Australia. E-mail: felipe.martelli@unimelb.edu.au*

Felipe Martelli, Thomas A. Ravenscroft Joint first authors.

a *School of BioSciences, The University of Melbourne, Melbourne, Victoria, Australia*

b *Janelia Research Campus, Howard Hughes Medical Institute, Ashburn, VA, USA*

nAChRα1, nAChRα2, nAChRα3, nAChRα4, nAChRβ1, nAChRβ2 and nAChRβ3,[9–11] whilst spinosad targets nAChRα6.[12,13] An imidacloprid dose of 2.5 ppm creates a long-lasting low Ca^{2+} flux into neurons expressing nAChRs, further reducing their cholinergic response by more than two-fold. Elevated Ca^{2+} levels likely explain the observed generation of reactive oxygen species (ROS) and mitochondrial stress in the CNS.[6] In contrast, exposure to 2.5 ppm spinosad prevents Ca^{2+} flux into neurons expressing *nAChRα6*. Blocked receptors are rapidly endocytosed[14] and shuttled to lysosomes, where spinosad likely accumulates.[7] Lysosomal dysfunction emerges within 2 h of exposure, followed by increased ROS levels and mitochondrial defects. Within 2 h of exposure to either imidacloprid or spinosad, oxidative stress spreads from the CNS to metabolic tissues, causing lipid stores to accumulate in the fat body and decrease in Malpighian tubules.[6,7] In adults, chronic exposure to 0.2 ppm spinosad or 4 ppm imidacloprid causes neurodegeneration and reduced vision acuity.[6,7] Flies pre-treated with the antioxidant *N*-acetylcysteine amide (NACA) show increased tolerance to both insecticides, supporting a causal role for ROS.[6,7]

To further dissect the downstream effects triggered by low doses of these insecticides, we performed RNA-sequencing (RNA-Seq) analyses on the brain and the fat body of *Drosophila* larvae exposed to 2.5 ppm spinosad for 2 h. Our findings were then compared to RNA-Seq analyses of the brain and fat body of larvae exposed to imidacloprid (2.5 ppm, 2 h) previously published by Martelli *et al.*[6] We also investigated *nAChRα6* expression by mining single-cell transcriptome data[15–17] and performed co-expression analyses for the genes enriched by spinosad exposure and the cells expressing spinosad targets. Both insecticides cause glutathione S-transferases (GSTs) and cytochromes P450 (P450s) gene families to be up-regulated in the brain and down-regulated in the fat body. However, spinosad has unique expression signatures linked to lysosomal function, protein folding, and male germline differentiation. Together with the *nAChRα6* expression analysis, these results led us to identify lysosomal dysfunction in the fat body of spinosad-exposed flies and reduced fertility of *nAChRα6* null males. This study underlines the value of using tissue-specific transcriptomics in studying the response of insects to insecticides.

2 MATERIALS AND METHODS

2.1 Fly strains and rearing

A susceptible isofemale line, Armenia#14, derived from Armenia#60 (Drosophila Genomics Resource Center #103394)[10] was used to perform transcriptomics and investigate the effect of insecticide exposure on lysosomal function in the fat body. To investigate the expression pattern of *nAChRα6* the progeny of a cross between *nAChRα6-T2A-Gal4* (BDSC #76137) and *UAS-mCD8::GFP* (BDSC #5130) were examined. The effects of *nAChRα6* loss of function on male fertility was assessed using a CRISPR knockout of *nAChRα6* (*nAChRα6 KO*) generated in the Canton-*S* genetic background.[18] Except where otherwise stated, experiments were conducted at 25 °C using standard fly media.[7]

2.2 Insecticide dilution and exposure

Dilutions of pure spinosad (Sigma Aldrich, St Louis, MO. USA) and pure imidacloprid (Sigma Aldrich), in dimethyl sulphoxide (DMSO), were used. Third instar larvae were exposed to a 2.5 ppm dose of insecticide (or DMSO for controls) for 2 h in NUNC cell plates (Thermo-Fisher Scientific, Waltham, MA, USA) containing 5% sucrose solution.[6,7]

2.3 Brain and fat body RNA isolation and transcriptome analyses of spinosad-exposed larvae

Three biological replicates were prepared per tissue (brain and fat body) per treatment (exposed group – 2.5 ppm spinosad for 2 h, and control group). Each replicate consisted of 40 brains or 40 fat bodies from third instar larvae. Samples were collected in 800 µL TRIsure (Bioline, Gregory Hills, NSW, Australia) and isolated following manufacturer's instructions. Prior to RNA library preparation, RNA was treated with RQ1 RNase-free DNase (Promega, Madison, WI, USA). RNA quality for each sample was tested by running a 1% agarose gel electrophoresis, and by spectrophotometry (NanoDrop ND-1000). All samples had at least 2 µg of total RNA, no signs of degradation and an optical density (OD) 260/280 ratio ≥ 1.9. Library preparation [250-300 bp complementary DNA (cDNA) insert], Illumina sequencing (150 bp paired end), and the analyses of the differentially expressed genes (DEGs) were carried out by Novogene Bioinformatics Technology in Singapore. Reads were aligned to the *Drosophila* genome and exons using Tophat2.[19] Reads representing gene transcripts were counted using HTSeq, and transcript per kilobase per million (TPM) was calculated for gene expression levels. Differential expression analysis was performed using DESeq2.[20] For significant DEGs, the adjusted (adj)-*P* value was set to $P < 0.05$.

2.4 Transcriptome analyses – brain and fat body of imidacloprid exposed larvae

The transcriptome analyses of the brain and fat body of third instar larvae exposed to 2.5 ppm imidacloprid for 2 h were first published by Martelli *et al.*[6] These data are used for comparison with the spinosad data presented here. Exposures to imidacloprid and spinosad were conducted in parallel and share the same control.

2.5 Gene Ontology (GO) and Kyoto Encyclopedia of Genes and Genomes (KEGG) pathway analyses

Transcriptomic data for each exposure condition (spinosad, imidacloprid, and control) and tissue of origin (brain or fat body) were examined to identify DEGs. DEGs with an adj-*P* value < 0.05 and expression fold change >|2| were selected and assigned Gene Ontology (GO) and Kyoto Encyclopedia of Genes and Genomes (KEGG) process using the software DAVID (2021 version).[21,22] GO and KEGG terms with a modified Fisher's exact *P*-value < 0.05 were then used to generate bar graphs and Venn diagrams using R (v.4.1.3, packages ggplot2 and ggVennDiagram).

2.6 Co-expression and single-cell transcriptome analysis of *nAChRα6* expression

Single-cell transcriptome analyses were performed using previously published data sets generated for the *Drosophila* larval brain[15] (GEO: GSE157202) and the adult brain[17] (GEO: GSE107451), fat body and testes[16] (https://flycellatlas.org/asap). Data were downloaded and processed using Seurat v3[23] applying the described parameters from the original publications and their assigned cell-specific markers to determine cluster identity. New clusters were made in the larval brain data using *para* expression to identify active neurons, *imp* expression for mature neurons, *pros* expression for immature neurons, *elav* expression for all neurons, *repo* for all glial cells, *alrm* for astrocytes, *wrapper* for cortex glia and *Indy* for surface glia.[15] Dot plots were generated by calculating the average expression of each gene in each cell type in a

defined cluster. Co-expression values for the larval brain, adult brain, and adult fat body were calculated by comparing the Pearson's co-expression value of *nAChRα6* with each gene from the spinosad transcriptome analyses in either all cells individually (All), or by calculating the mean expression of all cells in a cluster and comparing these values (Clusters). Feature plots for *nAChRα6* and *Ace* expression were obtained from scope.aertslab.org[17] using log transform, CPM normalization, and Expression-based plotting conditions.

2.7 Investigating insecticide impact on lysosomes

LysoTracker staining was used to investigate the impact of insecticide exposure on lysosomes[24] in the fat body of third instar larvae. After exposure to 2.5 ppm spinosad or imidacloprid for 2 h, larvae were dissected in Schneider's media (Thermo Fisher Scientific). Tissues were then transferred to phosphate-buffered saline (PBS) solution containing LysoTracker Red DND-99 (1:10000) (Thermo Fisher Scientific) for 3 min. After rinsing once in PBS, microscopy slides were mounted using Vectashield (Vector Laboratories). Images were obtained with a Leica TCS SP8 (DM600 CS), software LAS X. A total of six fat body samples were assessed per treatment. Using the software ImageJ, area occupied by lysosomes was measured in three different randomly chosen 2500 μm^2 sections per sample and these numbers averaged. Data were analysed using one-way analysis of variance (ANOVA) followed by Tukey's honestly significant difference (HSD) test.

2.8 Expression pattern of nAChRα6 in *Drosophila* larvae and adults

The *nAChRα6* expression pattern was assessed in the progeny of crosses between *nAChRα6-T2A-Gal4* (BDSC #76137) and *UAS-mCD8::GFP* (BDSC #5130). Tissues were dissected and fixed in 4% paraformaldehyde (PFA; Electron Microscopy Science) as previously reported.[25] Images were obtained with a Leica TCS SP8 (DM600 CS), software LAS X, and analysed in ImageJ.

2.9 Male fertility assay

The 4-day-old virgin Canton-*S nAChRα6 KO* males or Canton-*S* wild-type (WT) males were crossed to Canton-*S* WT virgin females. Males were individually housed, each with three virgins and allowed to mate for 2 days at 27 °C. Males were then transferred to a fresh vial (kept at 27 °C) with three new 4-day-old virgins each time being allowed to mate again for 2 days. At the end of the third mating period, the adults were discarded. Offspring (pupae) numbers were counted after 7 days. Data were analysed using one-way ANOVA followed by Tukey's HSD test. Only replicates where adults survived for the whole mating period were considered. At least 11 replicates were analysed per genotype. Experiments were conducted using molasses fly media.[7]

2.10 Investigation of adult testes

Canton-*S nAChRα6 KO* and Canton-*S* WT 8-day-old males were mated and kept under the same conditions used for the fertility assay. The size of seminal vesicles and ROS levels were assessed. To assess the size of seminal vesicles, testes were dissected in PBS and fixed in 4% PFA for 30 min at room temperature. Tissues were rinsed in PBS containing 0.1% Triton X-100, and then incubated with DAPI (4′,6-diamidino-2-phenylindole, final concentration 10 $\mu g\ mL^{-1}$) for 30 min. After rinsing in PBS microscopy slides were mounted in Vectashield (Vector Laboratories). To assess ROS levels, samples were stained with dihydroethidium (DHE) and mounted in Vectashield (Vector Laboratories).[7,26] Images were obtained with a Leica TCS SP8 (DM600 CS) using LAS X software. Seven samples per group were measured for DHE staining and five for DAPI staining. Data were quantified on ImageJ software and analysed using a Student's unpaired *t*-test.

3 RESULTS AND DISCUSSION

3.1 Low-dose exposures to spinosad affect genes involved in lysosomal function, protein folding, oxidative stress, metabolism of xenobiotics, and immunity

We began our analysis by comparing the transcriptome profiles of the brain and fat body of larvae exposed to 2.5 ppm spinosad for 2 h. Nine hundred and seventy-eight genes were exclusively up-regulated in the brain, and 963 in the fat body, whereas 146 were up-regulated in both tissues (adj-$P < 0.05$, fold change $> |2|$, Supporting Information Table S1) (Fig. 1(A)). Despite their physical proximity in the larva,[27] these tissues show distinct expression profiles after spinosad exposure even when, in some cases, they shared similar GO and KEGG pathway terms (Fig. 1(B),(C)).

The biological and metabolic processes associated with these genes in the brain involve the metabolism of xenobiotics by P450s, immune response, lipid metabolism, carbohydrate metabolism, amino acids metabolism, vitamin metabolism, protein folding and glutathione metabolism (Fig. 1(B)). The fat body is functionally analogous to the vertebrate liver and white adipose tissue[28] and is the centre for energy metabolism and innate immunity.[29] Processes up-regulated in the fat body are involved in energy production, carbohydrate metabolism, glutathione metabolism and protein folding (Fig. 1(C)).

Among the genes down-regulated by spinosad exposure, 345 were exclusive to the brain, 263 were exclusive to the fat body, and only 35 were common to both tissues (adj-$P < 0.05$; fold change $> |2|$) (Fig. 2(A)). The biological and metabolic processes associated with these genes in the brain involve morphogenesis and development, carbohydrate metabolism, immunity, and lysosomal function (Fig. 2(B)). Processes down-regulated in the fat body also involve terms related to morphogenesis, development, and immunity. Contrasting what happens in exposed brains, xenobiotic metabolism by P450s is down-regulated in exposed fat bodies (Fig. 2(C)).

In comparing the brain and fat body, exposure seems to cause distinct effects on energy metabolism. Different genes involved in pyruvate and citrate metabolism are up-regulated in each organ (Table S1). In the fat body, glycolysis/gluconeogenesis and the tricarboxylic acid (TCA) cycle seem to be up-regulated when compared to the brain (Fig. 1(B),(C)). In the fat body, little impact is observed for lipid metabolism genes. This reinforces the hypothesis that the lipid accumulation previously reported in this tissue is mainly the result of lipid deposit transfer from other tissues such as the Malpighian tubules,[6,7] with increased lipid droplet formation in the fat body deployed as a protective measure to prevent lipid peroxidation.[30] This may explain the down-regulation of terms related to P450s and glutathione metabolism in the fat body when compared to the brain.

P450s comprise a large multigene family that encodes a diverse class of heme-thiolate enzymes found in all insects.[31] Only a subset of the *Drosophila* P450 genes are well-characterized, but several have been implicated in xenobiotic detoxification.[32] Evidence of P450 mediated resistance to spinosad is limited and it cannot be assumed that every gene up-regulated here contributes to minimizing exposure impacts. The Malpighian tubules and midgut may be the primary sites of insecticide metabolism by P450s.[33] GSTs are a

Pest Management Science published by John Wiley & Sons Ltd on behalf of Society of Chemical Industry.

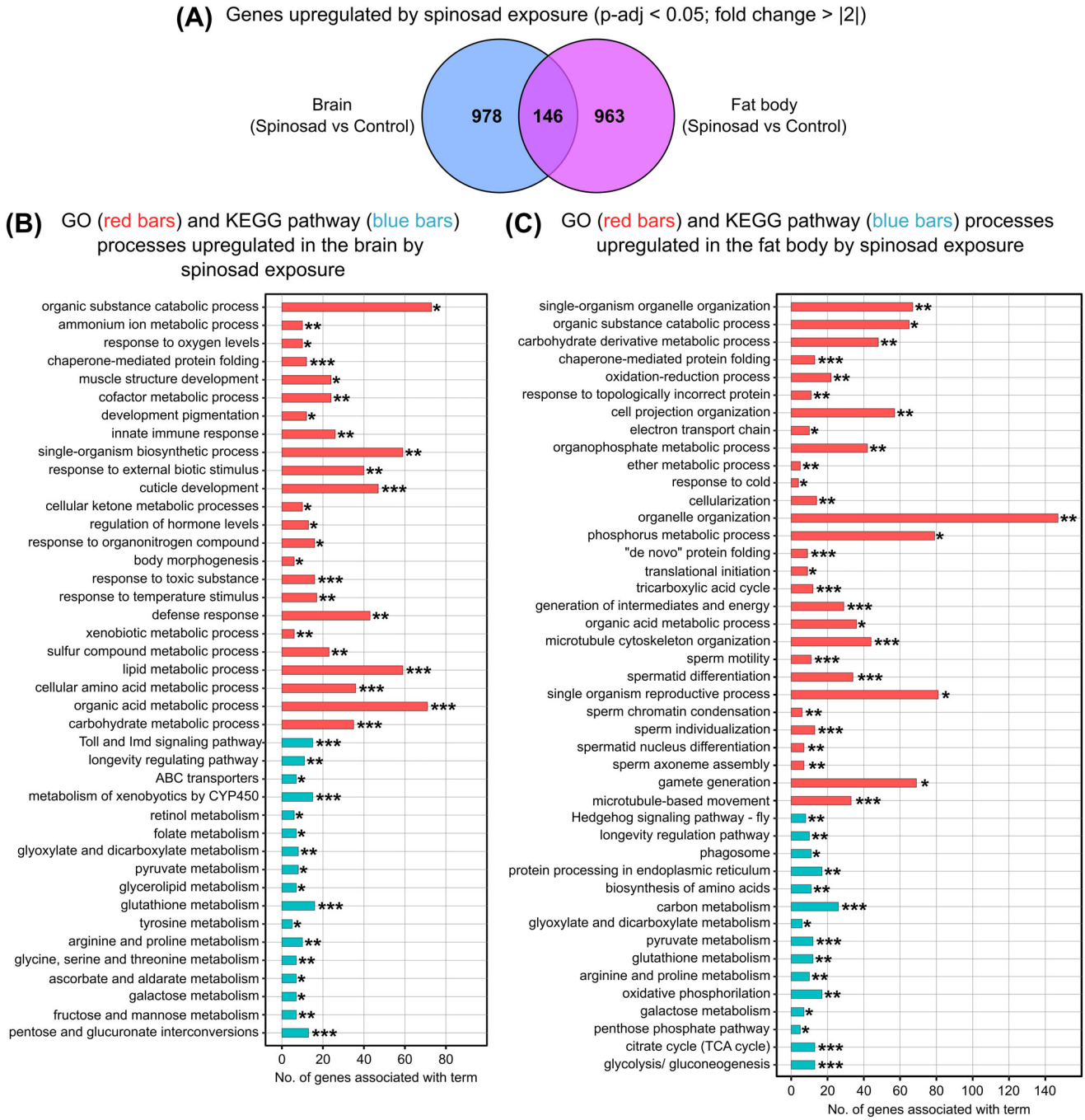

Figure 1. GO and KEGG pathway analyses of genes up-regulated in the brain and the fat body by spinosad exposure. *Drosophila* larvae exposed to 2.5 ppm spinosad for 2 h. (A) Number of genes exclusively up-regulated in each tissue and the number of overlapping genes between them (adj-$P < 0.05$; fold change > |2|). (B, C) Significant GO (red bars) and KEGG pathway (blue bars) processes up-regulated in the (B) brain and (C) fat body of spinosad-exposed larvae. Modified Fisher's exact test. *P-value < 0.05; **P-value < 0.01; ***P-value < 0.001.

conserved large family of enzymes known for metabolizing a wide range of endogenous and exogenous substrates.[34] GSTs are also important mediators in antioxidant response by conjugating electrophilic compounds to glutathione.[34] Increased GST activity has been correlated with resistance to all the major insecticide classes.[34,35] From the 35 genes encoding for GST enzymes in *Drosophila*, nine were up-regulated in the brain and ten down-regulated in the fat body (Table S1). The increased expression of GSTs in the brain is expected since this tissue harbours the target of spinosad and the accumulation of oxidative stress is first observed there.[7]

Several genes related to protein folding were up-regulated in the brain after spinosad exposure, while genes related to lysosome function were down-regulated (Figs 1 and 2, Supporting Information Fig. S1). Lysosomes are acidic organelles rich in hydrolytic enzymes which recycle a large number of cellular components.[36] Enlarged lysosomes are observed after a 2-h spinosad exposure, likely reflecting the trafficking of spinosad-blocked nAChRs to endocytic vesicles increasing the demand for lysosomal digestion in neurons.[7] In spinosad-exposed brains, a significant repression of the lysosomal α-mannosidase genes *LManIII*

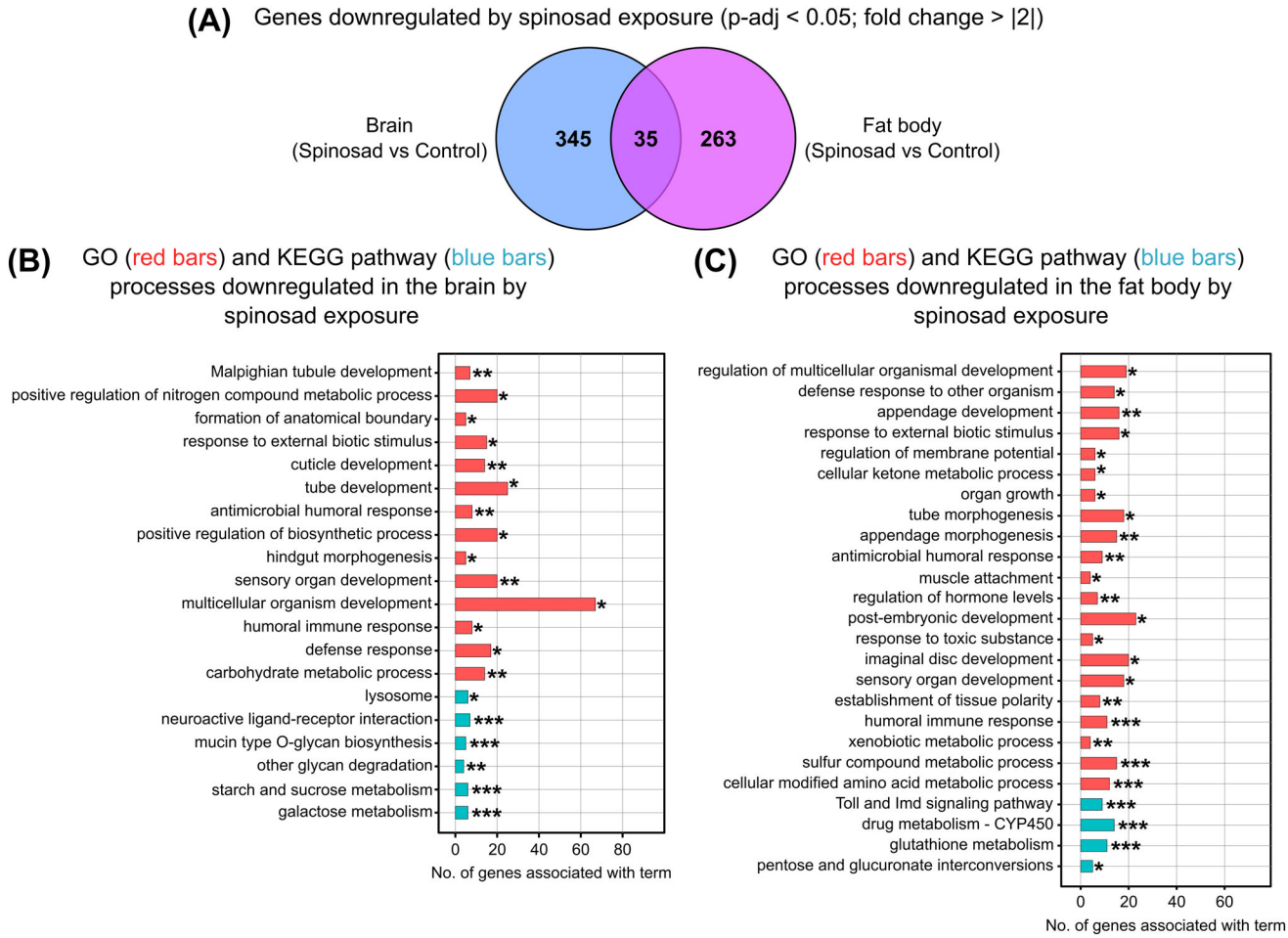

Figure 2. GO and KEGG pathway analyses of genes down-regulated in the brain and the fat body by spinosad exposure. *Drosophila* larvae exposed to 2.5 ppm spinosad for 2 h. (A) Number of genes exclusively down-regulated in each tissue and the number of overlapping genes between them (adj-$P < 0.05$; fold change > |2|). (B, C) Significant GO (red bars) and KEGG pathway (blue bars) processes down-regulated in the (B) brain and (C) fat body of spinosad-exposed larvae. Modified Fisher's exact test. *P-value < 0.05; **P-value < 0.01; ***P-value < 0.001.

(142-fold), *LManIV* (65-fold) and *LManV* (95-fold) is observed in comparison to unexposed brains (Table S1). This is indicative of the malfunctioning of lysosomal activity, resulting in the accumulation of undigested material that may cause brain cell death.[7] The activation of genes involved in protein folding suggests the accumulation of defective proteins, a process correlated with lysosomal dysfunction.[37]

3.2 The unique and the shared transcriptional signatures triggered by spinosad and imidacloprid

Next, we compared the brain transcriptome profiles of larvae exposed to spinosad *versus* those for larvae exposed to imidacloprid. The expression of 3359 genes is up-regulated by both insecticides (Table S1). Six hundred and eighty-six genes are up-regulated exclusively by spinosad and 96 by imidacloprid (adj-$P < 0.05$; fold change > |2|) (Fig. 3(A)). Spinosad exposure caused more genes involved in lipid and amino acid metabolism, response to stimulus, immunity, protein folding, and metabolism of glutathione and xenobiotics by P450s to be up-regulated in the brain (Fig. 3(B)). However, imidacloprid led to more genes involved in cuticle development, lysosomes, neuroreceptors, and carbohydrate metabolism being up-regulated (Fig. 3(C)).

When comparing the fat body transcriptome profiles 275 genes were up-regulated by spinosad, 236 up-regulated by imidacloprid, and 2891 shared between both treatments (adj-$P < 0.05$; fold change > |2|) (Fig. 4(A)). In the fat body, spinosad exposure led to the up-regulation of more genes involved with protein folding, morphogenesis, and development (Fig. 4(B)). Imidacloprid up-regulated more genes involved with lipid metabolism, immunity, and metabolism of xenobiotics by P450s (Fig. 4(C)).

It is important to stress that under the studied exposure conditions, imidacloprid does not significantly impact larval survival,[6] while spinosad kills over 95% of larvae.[7] Thus, when comparing the efficiency of these insecticides, the median lethal concentration (LC_{50}) of spinosad is 10–20 times lower than that of imidacloprid,[38] despite the dose of 2.5 ppm spinosad being approximately six-fold lower than 2.5 ppm imidacloprid when based on their molarity. These contrasting effects on survival are reflected in the expression profiles created by exposure to these chemicals. One of the most striking differences between them is the strong repression of genes involved in lysosome function and the up-regulation of protein folding genes in spinosad-exposed larvae.[6] This likely occurs because of the effects these insecticides have at low doses. Spinosad blocks nAChRα6 leading to the receptor recycle from neuronal membranes, triggering severe lysosomal disorder.[7] This is probably not overcome

Pest Management Science published by John Wiley & Sons Ltd on behalf of Society of Chemical Industry.

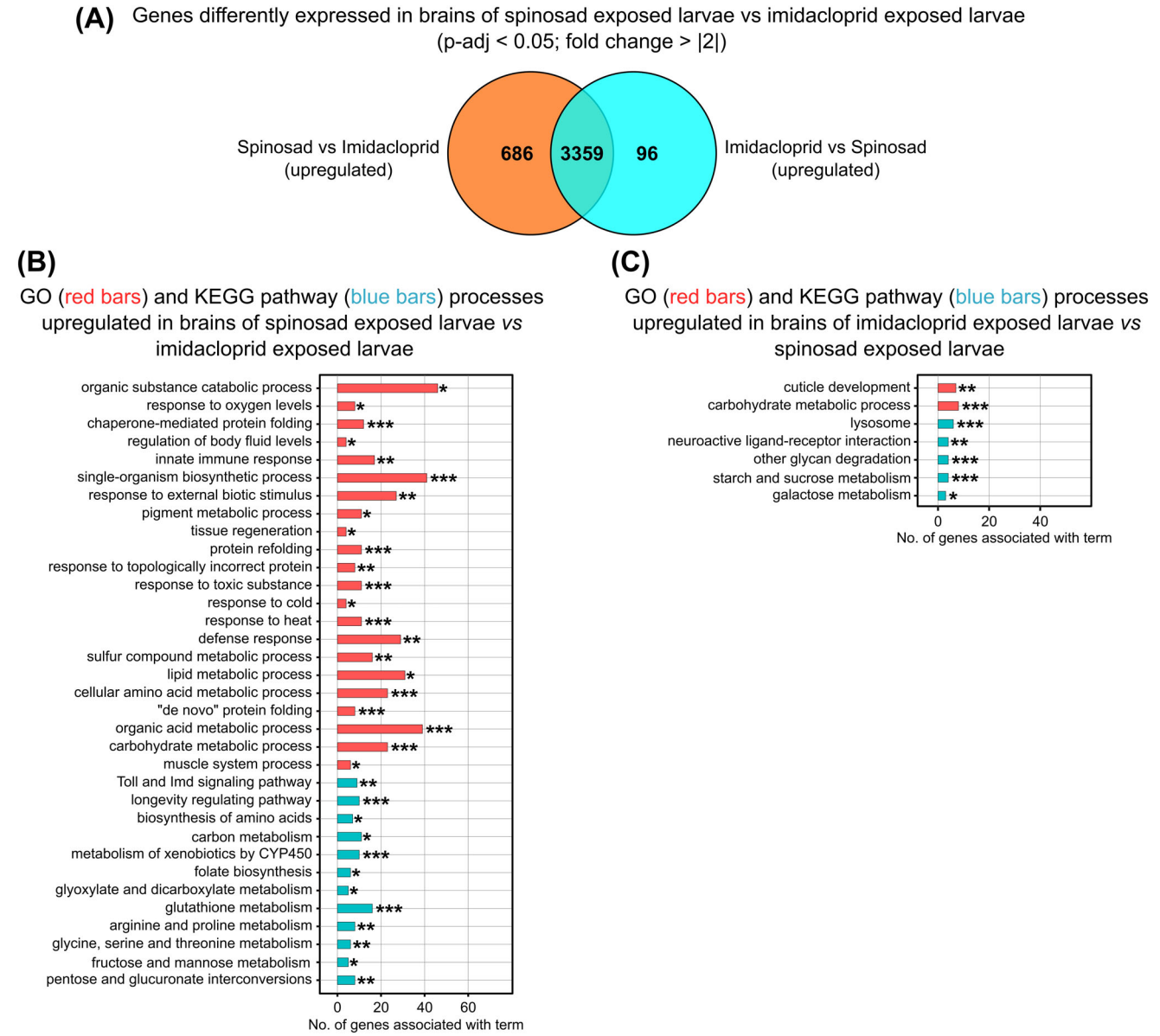

Figure 3. Comparative analyses of GO and KEGG pathway processes affected in the brain by spinosad exposure and imidacloprid exposure. *Drosophila* larvae exposed to 2.5 ppm spinosad or imidacloprid for 2 h. (A) Number of genes up-regulated for spinosad and imidacloprid exposures in the brain (adj-$P < 0.05$; fold change > |2|). (B, C) Significant GO (red bars) and KEGG pathway (blue bars) processes up-regulated in the brain of (B) spinosad-exposed and (C) imidacloprid-exposed larvae. Modified Fisher's exact test. **P*-value < 0.05; ***P*-value < 0.01; ****P*-value < 0.001.

by the larvae resulting in death. This phenomenon is absent following imidacloprid exposure, as it is rapidly metabolized and excreted.[39] Despite that, in the brains of imidacloprid-exposed larvae, a greater repression of antimicrobial peptide (AMP) genes is found compared to spinosad-exposed brains. The opposite effect is found in the fat body.

Our transcriptome analyses also draw attention to the higher number of similarities shared between the two insecticides (Figs 3 and 4), than between the two tissues (Figs 1 and 2). This reinforces that, despite the different modes of action, part of the low-dose damage revolves around a common denominator, these insecticides' capacity to produce oxidative stress.[6,7] It would be important to investigate whether similar transcriptional responses are evoked by other neurotoxic insecticides. It is also important to emphasize the additional information derived from examining the transcriptomes of key tissues, rather than those of whole animals where valuable information may be lost by pooling across all tissues.

3.3 The *nAChRα6* single cell expression and co-expression with genes enriched by spinosad exposure

We next asked whether the genes affected by spinosad exposure are commonly expressed in cells expressing the spinosad target, *nAChRα6*. We started by investigating *nAChRα6* expression using the available single-cell transcriptome data.[15–17] This analysis revealed that in the larval brain, *nAChRα6* is predominantly expressed in mature/active neurons and motor neurons, with little or no expression detected in the other cell types, such as glia (Fig. 5(A)–(C)). *Acetylcholine esterase* (*Ace*) is expressed in the same cell types as *nAChRα6* in the larval brain (Fig. 5(A)–(C)). *Ace* terminates impulse transmission by hydrolysis of acetylcholine, the

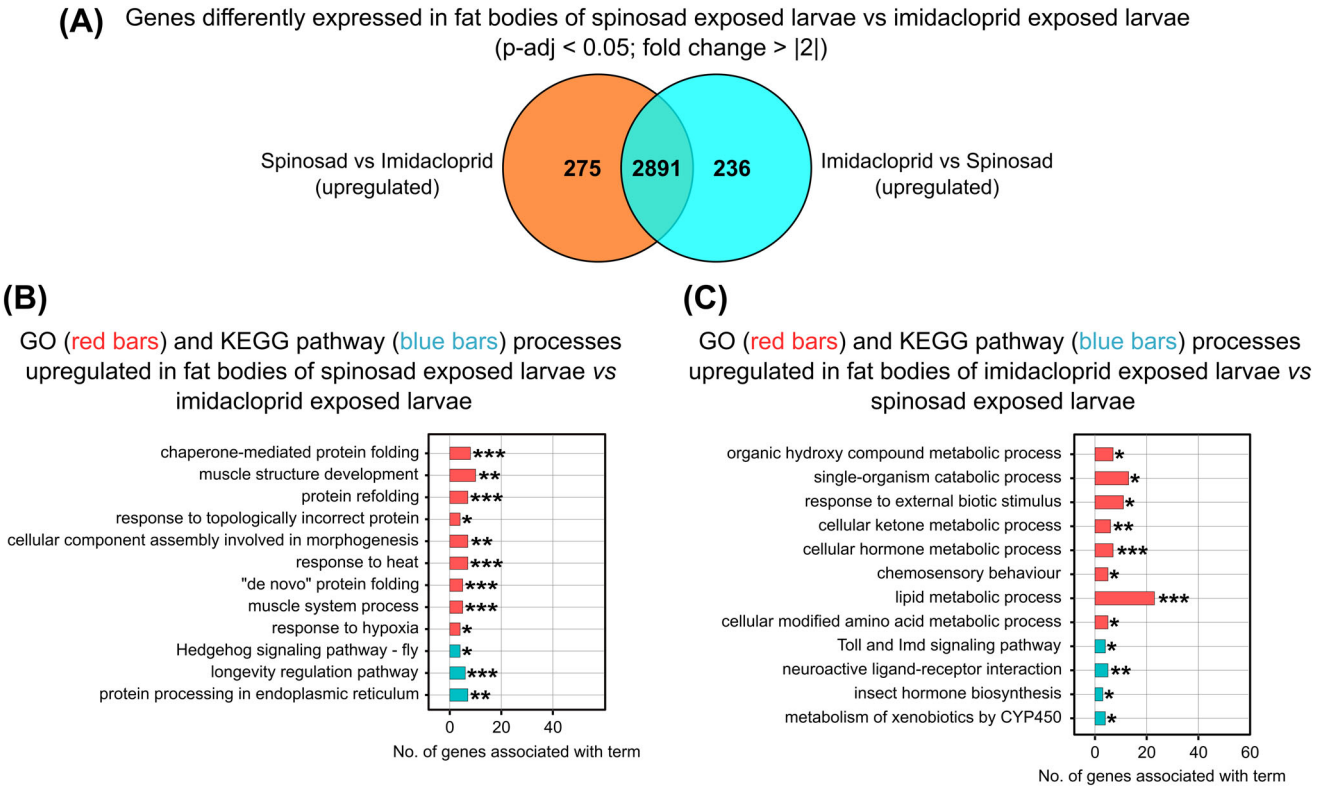

Figure 4. Comparative analyses of GO and KEGG pathway processes affected in the fat body by spinosad exposure and imidacloprid exposure. *Drosophila* larvae exposed to 2.5 ppm spinosad or imidacloprid for 2 h. (A) Number of genes up-regulated in the fat body with spinosad or imidacloprid exposure (adj-$P < 0.05$; fold change > |2|). (B, C) Significant GO (red bars) and KEGG pathway (blue bars) processes up-regulated in the fat body of (B) spinosad-exposed and (C) imidacloprid-exposed larvae. Modified Fisher's exact test. *P-value < 0.05; **P-value < 0.01; ***P-value < 0.001.

agonist of nAChRs, thus being required for proper functioning of nAChRs regardless of their subunit configuration. Surprisingly, the adult whole-body single-cell transcriptome[16] shows that *nAChRα6* is also expressed in a small number of fat body cells with noteworthy expression in the male germline accessory cells in the fat body (Fig. 5(D)–(F)), and in later-stage spermatocytes of the testes (Fig. S2). *Ace* expression in the fat body is sparser than that of *nAChRα6* (Fig. 5(D)–(F)), but comparable to *nAChRα6* expression in testes (Fig. S2). This indicates that cells expressing *nAChRα6* in the testes would be able to hydrolyse acetylcholine. Some level of expression of the other *nAChRs* is also found in the fat body (Fig. 5(F)). Spinosad's classification as a neurotoxin is contingent on its target's localization to the brain. *nAChRα6* expression outside of the CNS suggests a potential for spinosad to target other tissues. It was important to consider whether some level of tissue contamination present in the single-cell data could also explain part of these results, but these cells do not express neuronal or glial cell markers.[16] It is noteworthy that in the fat body (Fig. 5(F)), among all nAChRs subunits, *nAChRα1* shows the most similar expression patter to that of *Ace*, according to the single cell data.[16] However, *nAChRα6* appears to share a similar expression pattern to that of *nAChRα5*.[16] *nAChRα5* and *nAChRα6* are not known to be co-expressed. The contrast in how the expression patterns of *nAChRs* and *Ace* genes compare against each other in these two tissues (Fig. 5(C),(F)) suggests differences in their regulation and biological role between the fat body and the brain.

To test if the genes perturbed by spinosad are commonly expressed in the same cells that express spinosad target *nAChRα6*, we investigated a list of 116 enriched selected genes from the transcriptome of spinosad-exposed larvae. These genes (Table S2) are involved with endocytosis, lysosome function, proteasome-mediated protein degradation [ubiquitin-proteasome system (UPS)], oxidative response, lipid metabolism, xenobiotic metabolism, and immunity. In the brain, in most cases, no positive expression correlation was found between these genes and *nAChRα6* (Tables 1 and S2). This could mean that, (a) spinosad creates enough perturbation to shift expression profiles of target cells, and/or (b) the major perturbations observed in the transcriptome profiles of exposed brains come from non-target cells. To test hypothesis (b) we investigated whether the genes in our list are commonly expressed in all neurons, all glial cells, astrocytes, cortex glia, or surface glia (Table S2). Glia, particularly surface glial cells, showed a positive correlation with the genes involved in lysosome function, UPS and especially oxidative response, xenobiotic metabolism, and immunity. That is not surprising given that glial cells have been shown to make a vital contribution to the deleterious accumulation of ROS in neurons.[40,41] Glia perform vital roles, providing support and protection for neurons and cleansing metabolites and toxic compounds generated by neuronal activity.[42] Our results suggest that at least part of spinosad's impacts on targeted *nAChRα6* cells in the brain spills over to glial cells. This could explain some of the changes in gene expression profiles in brains of exposed larvae. It is also noteworthy that the same 116 genes generally show positive expression correlation with *nAChRα6* in the fat body (Table 1).

Pest Management Science published by John Wiley & Sons Ltd on behalf of Society of Chemical Industry.

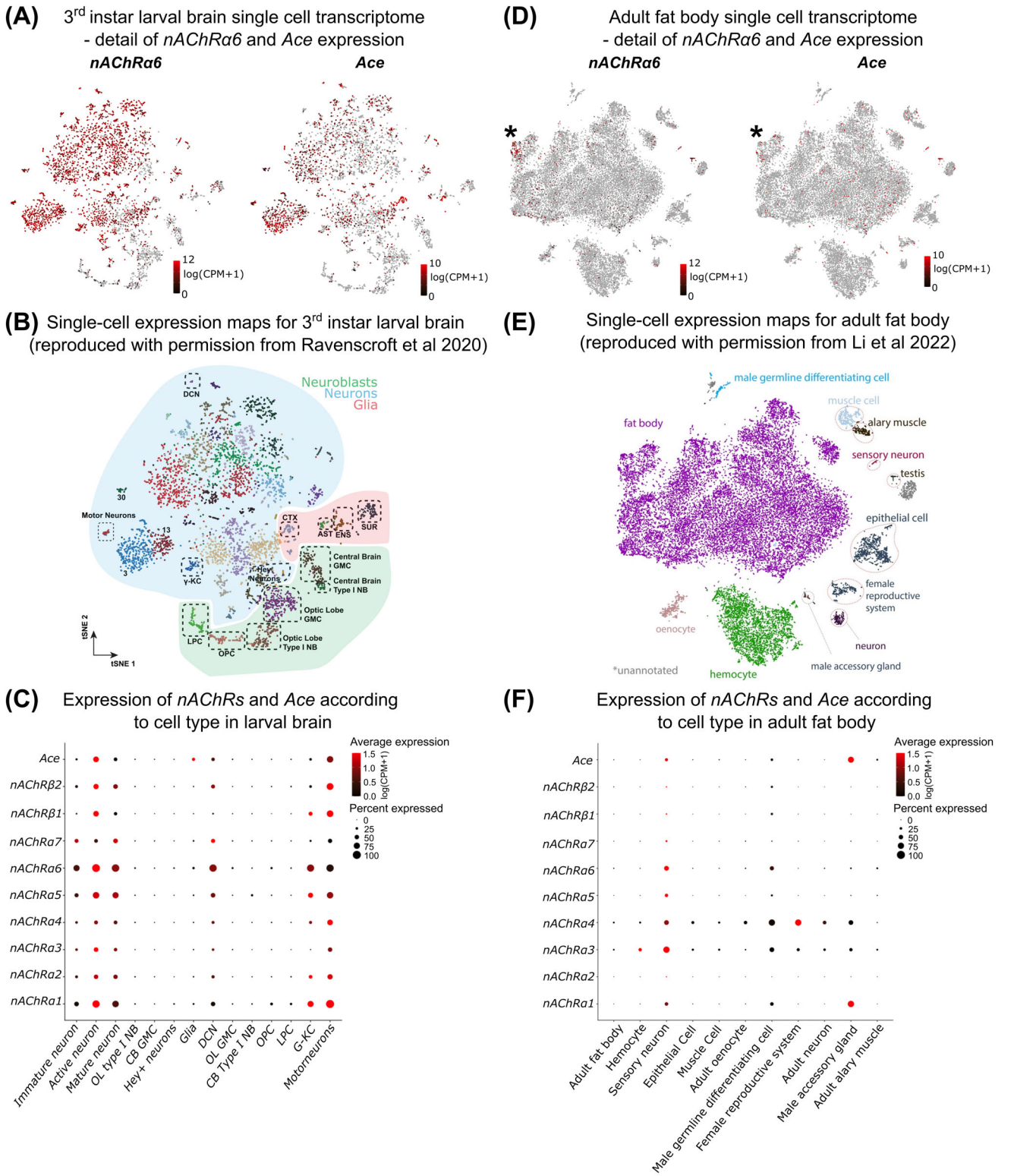

Figure 5. The *nAChRα6* and *Ace* expression according to the single-cell transcriptome. (A) Detail of *nAChRα6* and *Ace* expression in third instar larval brain single cell transcriptome.[15] (B) Annotated cell clusters in third instar larval brain.[15] (C) The *nAChRα6* expression is restricted to mature neurons, specifically motor neurons, Gamma Kenyon Cells (G-KC), and Dorsal Cluster Neurons (DCN). The expression of *nAChRα6* is similar to *Ace*. (D) Detail of *nAChRα6* and *Ace* expression in adult fat body single cell transcriptome.[16] (E) Annotated cell clusters in adult fat body.[16] (F) In the fat body *nAChRα6* is expressed in sensory neurons, and in male germline differentiating cells (marked with *). Expression of the other *nAChR* subunits in the fat body shows that non-neuronal expression of *nAChR* is also apparent. *Ace* is expressed in the same cell types as *nAChRα6* in the adult fat body. Red-black colour scale represents minimum–maximum normalized log(CPM + 1) gene expression and a size scale (percentage expressed) represents the number of cells in each cluster expressing the given gene. LPC, lamina precursor cells; OPC, outer proliferation centre; NB, neuroblast; CB, central brain; GMC, ganglion mother cells; CPM, counts per million.

Pest Management Science published by John Wiley & Sons Ltd on behalf of Society of Chemical Industry.

Table 1. The *nAChRα6* co-expression with differentially expressed genes in response to spinosad

		Brain – spinosad			Fat body – spinosad			*nAChRα6* Correlation	
Flybase identifier	Gene	Response	Fold change	Adj *P*-value	Response	Fold change	Adj *P*-value	Brain clusters (larva)	Fat body clusters (adult)
Endocytosis									
FBgn0013278	*Hsp70Bb*	↑	7.88	4.36E-86	↑	33.13	1.83E-22	−0.23	0.64
FBgn0001230	*Hsp68*	↑	18.83	0	↑	3.53	5.02E-14	−0.35	0.00
Lysosomes									
FBGN0032069	*LManVI*	↓	−94.74	0				−0.18	0.88
FBGN0039800	*Npc2g*	↑	7.35	1.17E-128				−0.22	0.16
Proteasome-mediated ubiquitin-dependent protein catabolic process									
FBgn0034484	*CG11044*	↑	4.03	4.87E-06				NA	0.33
FBgn0039667	*CG2010*	↑	3.54	2.53E-32				0.25	0.22
FBgn0050156	*CG30156*				↑	2.91	2.59E-05	0.40	0.26
FBgn0054025	*CG34025*				↑	3.17	0.01712	NA	0.22
Oxidative stress response									
FBgn0010040	*GstD4*				↓	−5.81	9.20E-13	−0.32	0.45
FBgn0010041	*GstD5*	↑	2.54	9.25E-04	↓	−5.81	9.76E-19	−0.23	0.29
FBgn0010043	*GstD7*	↑	8.51	6.04E-89				−0.23	0.37
FBgn0063491	*GstE9*	↑	6.42	4.47E-101				−0.01	0.15
Lipid metabolism									
FBgn0039471	*CG6295*				↓	−9.82	0.00152	NA	0.54
FBgn0087002	*apolpp*	↑	8.23	0				0.051	−0.08
FBgn0032136	*Apoltp*	↑	10.17	0				0.63	0.11
Xenobiotic metabolism (P450s)									
FBgn0031182	*Cyp6t1*	↓	−5.18	0.03343	↓	−15.76	9.08E-05	−0.22	0.68
FBgn0033065	*Cyp6w1*	↑	6.88	0				0.04	0.21
FBgn0000473	*Cyp6a2*	↑	6.23	9.22E-109				0.22	0.78
FBgn0033978	*Cyp6a23*				↓	−3.72	0.03679	−0.32	0.22
Immune response									
FBgn0004240	*Diptericin A*	↓	−27.81	1.14E-18	↓	−263.09	9.58E-05	−0.06	0.06
FBgn0052279	*Drsl2*	↓	−73.57	1.65E-219				0.07	0.18
FBgn0052185	*edin*				↓	−105.18	1.40E-04	−0.19	−0.08

Note: Larval brain and larval fat body transcriptome analyses. Top impacted genes by spinosad exposure (↓ gene down-regulated; ↑ gene up-regulated). Pearson's correlation of *nAChRα6* expression refers to the average expression of each gene in the same cell types, defined by cluster annotation. Pearson's correlation color code: (green) positive correlation; (pink) negative correlation; (white) no correlation (values rounded to two decimal, complete dataset in Supporting Information Table S2).

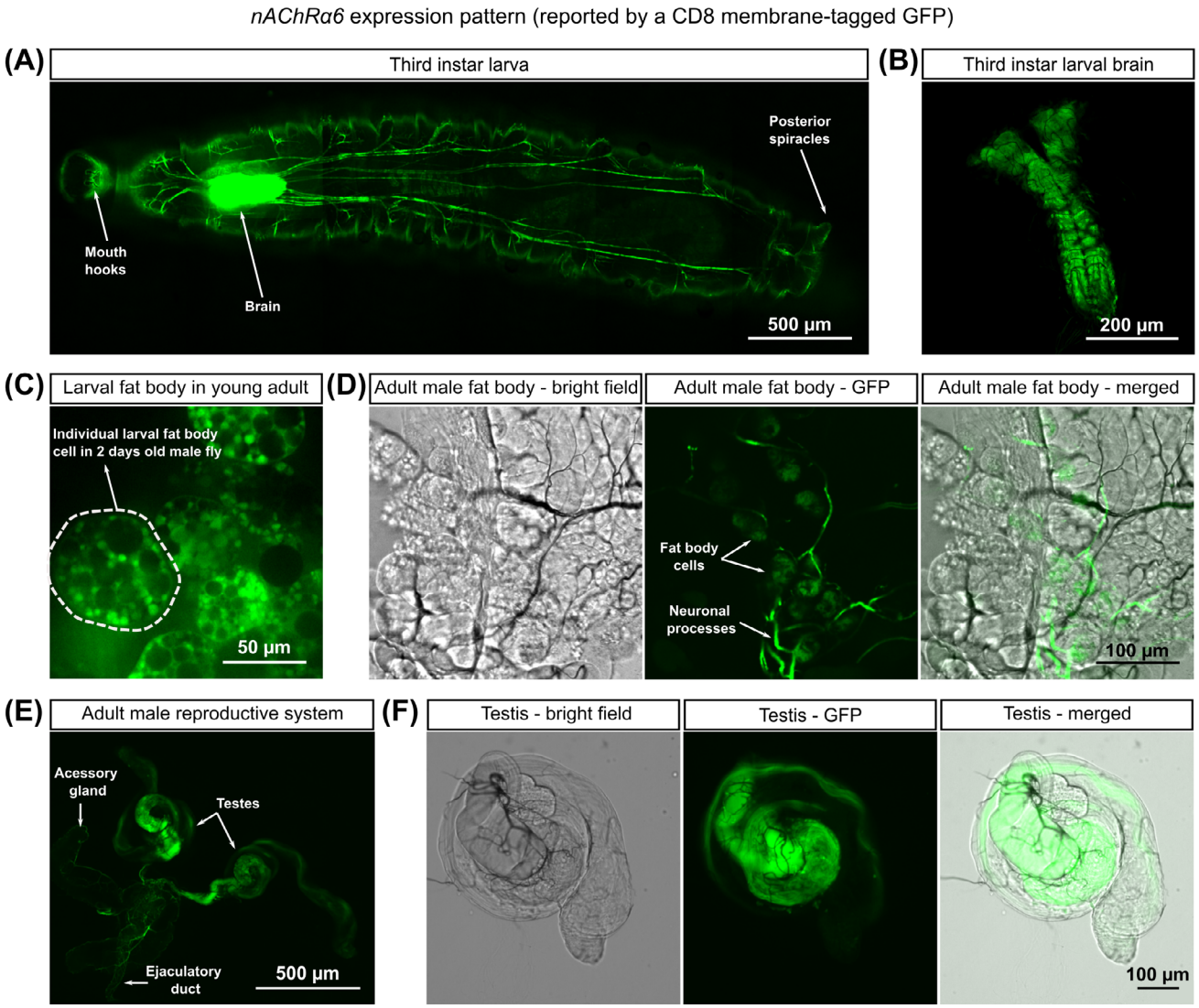

Figure 6. Expression pattern of *nAChRα6*. The *nAChRα6-T2A-Gal4* (BDSC #76137) driving the expression of *UAS-mCD8::GFP* (BDSC #5130). (A) High expression levels of *nAChRα6* are observed in third instar larval neuronal tissue, but not elsewhere. (B) Detail of *nAChRα6* expression in third instar larval brain. (C) High-level expression of *nAChRα6* observed in the larval fat body cells present in 2-days old adult male. (D–F) The *nAChRα6* expression in 7-day-old adult male (D) fat body, (E) reproductive system, and (F) testis.

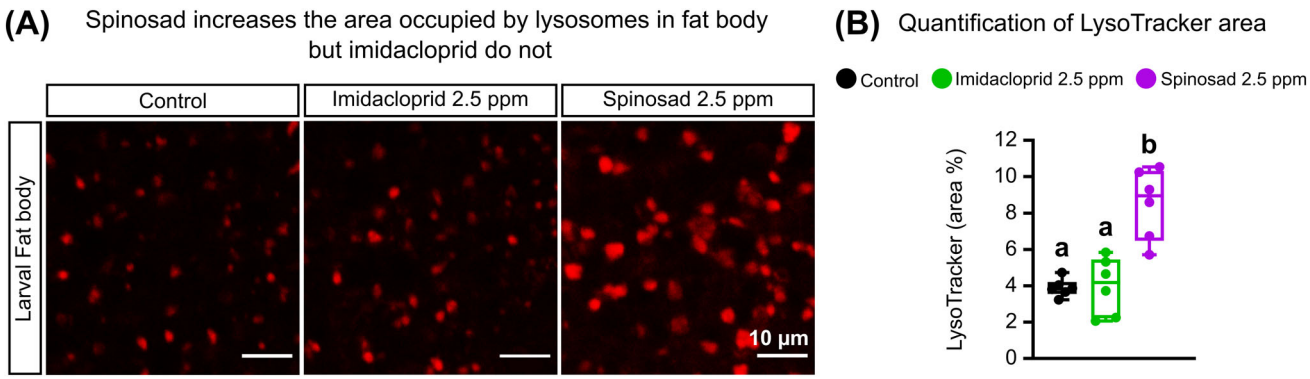

Figure 7. Spinosad leads to the accumulation of larger lysosomes in the fat body. Larvae exposed to 2.5 ppm of either imidacloprid or spinosad for 2 h. (A) LysoTracker staining of acidic organelles (lysosomes) in fat bodies. (B) Quantification of the area occupied by lysosomes in fat body sections of 50 µm × 50 µm ($n = 6$ larvae per treatment, three sections per larva). One-way ANOVA followed by Tukey's HSD test; different letters (a and b) represent statistically significant differences ($P < 0.01$).

3.4 The *nAChRα6* expression outside of the central nervous system and the impact of spinosad

The detection of *nAChRα6* expression in fat body and testes[16] (Figs 5(D)–(F) and S2) and the presence of GO terms related to male reproduction in transcriptome profiles of spinosad-exposed larvae (Fig. 1(C)), prompted us to further investigate these tissues. Using a membrane green fluorescent protein (GFP) reporter we verified *nAChRα6* expression in *Drosophila* larvae and adult males. Whereas no clear *nAChRα6* expression was observed in non-neuronal larval tissues (Figs 6(A),(B) and S3), in 2-day-old adult males *nAChRα6* expression was found in the remnant larval fat body cells (Fig. 6(C)). During metamorphosis, the larval fat body dissociates forming individual spherical, free-floating cells, that fuel metamorphosis, and eventually die when adults reach 3-day-old.[43,44] The adult fat body showed a low level of *nAChRα6* expression (Fig. 6(D)), as expected based on the adult single-cell transcriptome data. In the male reproductive system, *nAChRα6* seems to show strong expression in germline cells, once again confirming the adult single-cell transcriptome data[16] (Fig. 6(F)). Expression of other nAChRs subunits (α1, α2, β1, and β2) has been reported in male ejaculatory duct neurons.[9]

Though *nAChRα6* expression was not detected in third instar larval fat bodies using the GFP reporter, its expression in this tissue at other life stages (Fig. 6(C),(D)) led us to investigate whether spinosad could trigger lysosomal defects. As in the larval brain, exposure to 2.5 ppm spinosad[7] caused lysosome enlargement in larval fat body. The average 2.2-fold increase in the area occupied by lysosomes (Fig. 7) is suggestive of lysosomal storage disease,[36] known to create mitochondrial instability and generate ROS.[45,46] This phenomenon could disrupt fat body function and contribute to an energy imbalance. Exposure to imidacloprid under the same conditions did not affect the area occupied by lysosomes (Fig. 7).

Following the *nAChRα6* expression detected in the testes (Figs 6 (E),(F) and S2), we investigated the effects of *nAChRα6* loss of function in male fertility (Fig. 8). We found that 8-to-10-day-old mutant males show a drastic reduction in the number of offspring produced in comparison to WT males ($P < 0.0001$) (Fig. 8(A)). The *nAChRα6* loss of function has been connected to increased oxidative stress by genome-wide association studies[47] and ROS

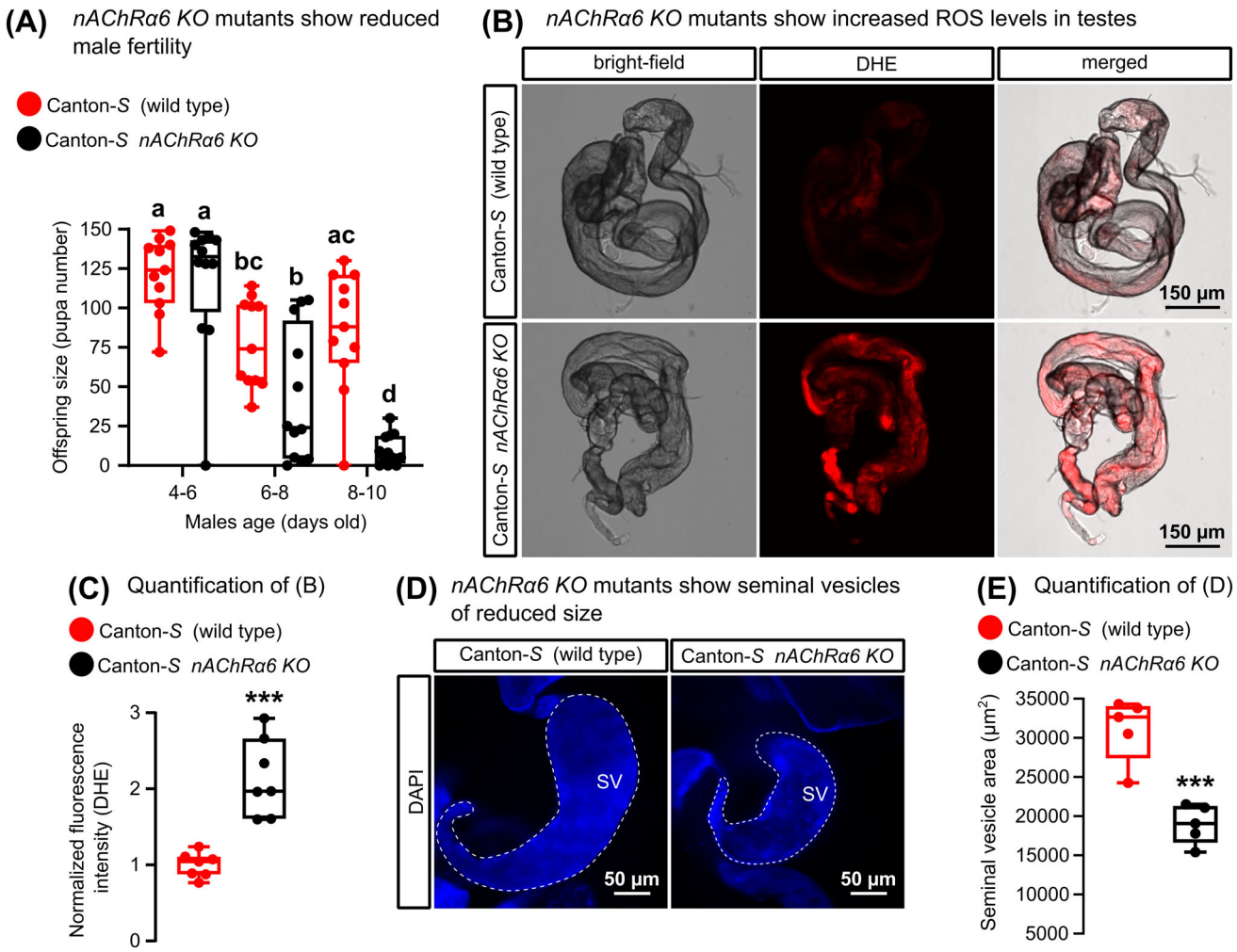

Figure 8. The *nAChRα6 KO* mutants show reduced fertility and increased oxidative stress. (A) Offspring number produced by non-exposed *nAChRα6 KO* or Canton-*S* WT males crossed with Canton-*S* WT females. At least 11 replicates per genotype. One-way ANOVA followed by Tukey's HSD test; different letters (a, b, c, and d) represent statistically significant differences ($P < 0.05$). (B) Levels of ROS measures by DHE staining in testes of 8-day-old non-exposed *nAChRα6 KO* or Canton-*S* WT males. (C) Quantification of (B) in terms of normalized fluorescence intensity ($n = 7$ samples/genotype). (D) Size of the seminal vesicles of 8-day-old non-exposed *nAChRα6 KO* or Canton-*S* WT males. (E) Quantification of (D) in terms of seminal vesicle area in µm^2 ($n = 5$ samples/genotype). Student's unpaired *t*-test; ***P-value < 0.001.

Pest Management Science published by John Wiley & Sons Ltd on behalf of Society of Chemical Industry.

staining[7] in the brain. Thus, we investigated oxidative stress in the testes of 8-day-old mutants and found an average two-fold increase in ROS levels compared to WT males (Fig. 8(B),(C)). Mutants also showed an average 40% reduction in the size of seminal vesicles (Fig. 8(D),(E)). These phenotypes add to a number of other impacts previously described in *nAChRα6* loss of function mutants – reduced longevity of virgin female flies, defects in visual acuity, a mild but significantly higher level of ROS in the brain, and higher levels of lipid stores in the fat body and hemolymph.[7] The reduced seminal vesicle size and fertility of mutants found here could be a consequence of the increased oxidative stress in the testes.[48] Here, we first demonstrate a clear link between *nAChRα6* loss of function and reduced male fertility. No fitness costs have been observed in *nAChRα6* null females.[49] The *nAChRα6* associated resistance to spinosad has been found in the field in many species.[50–54] The data presented here indicate that resistance in males should be examined for impacts on reproduction.

4 CONCLUSIONS

The widespread use of insecticides creates the potential for non-target organisms, including non-pest insects to be exposed.[2,55] Low-dose concentrations of these chemicals can affect behaviour, fitness, and development of target and non-target insects.[56] The low doses studied here caused up-regulation of P450 and GST genes in the brain and down-regulation in the fat body. Both insecticides seemed to increase the energetic demand of the fat body more than the brain, with a greater activation of genes related to glycolysis/gluconeogenesis and TCA cycle. Genes encoding AMPs were among the most strongly down-regulated in the brain and even more so in fat body of spinosad-exposed flies, suggesting the potential for increased susceptibility to pathogens and parasites. Transcriptome analysis of other tissues, such as the midgut, Malpighian tubules, testes, and hemolymph are likely to reveal other tissue-specific profiles. Fat body transcriptome profiles of spinosad-exposed larvae also revealed disturbance of genes involved in protein folding. This was further connected to the onset of lysosome dysfunction in fat body following spinosad exposure. And following the suggestion of disturbance of genes involved in reproduction, we detected reduced fertility of *nAChRα6* loss of function males, uncovering a potential fitness cost for the target-site spinosad resistant mutation.[50–54] Together, gene expression changes paint a broad picture that greatly aligns with the physiological [oxidative stress and reduced adenosine triphosphate (ATP) levels] and morphological (changes in lipid deposits across different tissues and neurodegeneration) impacts observed under low dose acute and chronic exposures.[6,7] Many other insecticide classes have been shown to produce markers of oxidative stress.[57–59] ROS may be a key element of their mode of action at low doses. If true, a ROS-induced mechanism of action might be shared among a vast range of pesticides to which beneficial insects are unintentionally exposed. Tissue-specific transcriptomics and single-cell transcriptome data used here could be valuable tools to help dissect the low-dose mode of action of these insecticides. The increased accessibility and use of spatial transcriptomics methods[60] will offer even greater power to examine insecticide impacts within and between tissues.

ACKNOWLEDGEMENTS

FM was supported by a Victorian Latin America Doctoral Scholarship, an Alfred Nicholas Fellowship, a University of Melbourne Faculty of Science Travelling Scholarship, and The Robert Johanson and Anne Swann Fund – Native Animals Trust. TAR was supported by the Howard Hughes Medical Institute. WH received a Commonwealth supported place (CSP). PB was supported by the University of Melbourne. The authors thank Trent Perry for helpful advice in the conduct of this research. Open access publishing facilitated by The University of Melbourne, as part of the Wiley - The University of Melbourne agreement via the Council of Australian University Librarians.

DATA AVAILABILITY STATEMENT

RNA-Seq data has been deposited with links to BioProject accession number PRJNA603631 in the National Centre for Biotechnology Information (NCBI) BioProject database.

SUPPORTING INFORMATION

Supporting information may be found in the online version of this article.

REFERENCES

1 Lasram MM, Dhouib IB, Annabi A, El Fazaa S and Gharbi N, A review on the molecular mechanisms involved in insulin resistance induced by organophosphorus pesticides. *Toxicology* **322**:1–13, Elsevier Ireland Ltd (2014).
2 Yadav I, Devi N, Syed J, Cheng Z, Li J, Zhang G *et al.*, Science of the Total environment current status of persistent organic pesticides residues in air, water, and soil, and their possible effect on neighboring countries: a comprehensive review of India. *Sci Total Environ* **511**:123–137, Elsevier BV (2015).
3 Scott JG and Buchon N, *Drosophila melanogaster* as a powerful tool for studying insect toxicology. *Pestic Biochem Physiol* **161**:95–103, Elsevier Inc (2019).
4 Duzguner V and Erdogan S, Acute oxidant and inflammatory effects of imidacloprid on the mammalian central nervous system and liver in rats. *Pestic Biochem Physiol* **97**:13–18, Elsevier Inc (2010).
5 van Klink R, Bowler DE, Gongalsky KB, Swengel AB, Gentile A and Chase JM, Meta-analysis reveals declines in terrestrial but increases in freshwater insect abundances. *Science* **368**:417–420 (2020).
6 Martelli F, Zhongyuan Z, Wang J, Wong C-O, Karagas NE, Roessner U *et al.*, Low doses of the neonicotinoid insecticide imidacloprid induce ROS triggering neurological and metabolic impairments in drosophila. *Proc Natl Acad Sci* **117**:25840–25850 (2020).
7 Martelli F, Hernandes NH, Zuo Z, Wang J, Wong C-O, Karagas NE *et al.*, Low doses of the organic insecticide spinosad trigger lysosomal defects, elevated ROS, lipid dysregulation, and neurodegeneration in flies. *Elife* **11**:1–33 (2022).
8 Breer H and Sattelle DB, Molecular properties and functions of insect acetylcholine receptors. *J Insect Physiol* **33**:771–790 (1987).
9 Ihara M, Furutani S, Shigetou S, Shimada S, Niki K, Komori Y *et al.*, Cofactor-enabled functional expression of fruit fly, honeybee, and bumblebee nicotinic receptors reveals picomolar neonicotinoid actions. *Proc Natl Acad Sci U S A* **117**:16283–16291 (2020).
10 Perry T, Heckel DG, McKenzie JA and Batterham P, Mutations in Dα1 or Dβ2 nicotinic acetylcholine receptor subunits can confer resistance to neonicotinoids in *Drosophila melanogaster*. *Insect Biochem Mol Biol* **38**:520–528 (2008).
11 Komori Y, Takayama K, Okamoto N, Kamiya M, Koizumi W, Ihara M *et al.*, Functional impact of subunit composition and compensation on Drosophila melanogaster nicotinic receptors–targets of neonicotinoids, ed. by Palli SR. *PLOS Genet* **19**:e1010522 (2023).
12 Perry T, Somers J, Yang YT and Batterham P, Expression of insect α6-like nicotinic acetylcholine receptors in Drosophila melanogaster highlights a high level of conservation of the receptor: Spinosyn interaction. *Insect Biochem Mol Biol* **64**:106–115, Elsevier Ltd (2015).
13 Perry T, McKenzie JA and Batterham P, A Dα6 knockout strain of Drosophila melanogaster confers a high level of resistance to spinosad. *Insect Biochem Mol Biol* **37**:184–188 (2007).

14 Nguyen J, Ghazali R, Batterham P and Perry T, Inhibiting the proteasome reduces molecular and biological impacts of the natural product insecticide, spinosad. *Pest Manag Sci* **77**:3777–3786 (2021).
15 Ravenscroft TA, Janssens J, Lee P-T, Tepe B, Marcogliese PC, Makhzami S *et al*., Drosophila voltage-gated sodium channels are only expressed in active neurons and are localized to distal axonal initial segment-like domains. *J Neurosci* **40**:7999–8024 (2020).
16 Li H, Janssens J, De Waegeneer M, Kolluru SS, Davie K, Gardeux V *et al*., Fly cell atlas: a single-nucleus transcriptomic atlas of the adult fruit fly. *Science* **375**:1–25 (2022).
17 Davie K, Janssens J, Koldere D, De Waegeneer M, Pech U, Kreft Ł *et al*., A single-cell transcriptome atlas of the aging drosophila brain. *Cell* **174**:982–998.e20 (2018).
18 Luong HNB, *In Vivo Functional Characterization of Nicotinic Acetylcholine Receptors in Drosophila Melanogaster*. The University of Melbourne, Melbourne, Australia (2018).
19 Kim D, Pertea G, Trapnell C, Pimentel H, Kelley R and Salzberg SL, TopHat2: accurate alignment of transcriptomes in the presence of insertions, deletions and gene fusions. *Genome Biol* **14**:R36 (2013).
20 Love MI, Huber W and Anders S, Moderated estimation of fold change and dispersion for RNA-seq data with DESeq2. *Genome Biol* **15**:550 (2014).
21 Huang DW, Sherman BT and Lempicki RA, Systematic and integrative analysis of large gene lists using DAVID bioinformatics resources. *Nat Protoc* **4**:44–57 (2009).
22 Sherman BT, Hao M, Qiu J, Jiao X, Baseler MW, Lane HC *et al*., DAVID: a web server for functional enrichment analysis and functional annotation of gene lists (2021 update). *Nucleic Acids Res* **50**:W216–W221, Oxford University Press (2022).
23 Stuart T, Butler A, Hoffman P, Hafemeister C, Papalexi E, Mauck WM *et al*., Comprehensive integration of single-cell data. *Cell* **177**:1888–1902.e21, Elsevier Inc (2019).
24 Martelli F, In vivo assessment of lysosomal stress in the drosophila brain using confocal fluorescence microscopy. *Bio Protoc* **13**:1–9 (2023).
25 Martelli F, Evaluation of mitochondrial turnover using fluorescence microscopy in drosophila. *Bio Protoc* **12**:1–11 (2022).
26 Owusu-Ansah E, Yavari A and Banerjee U, A protocol for in vivo detection of reactive oxygen species. *Nat Protoc*:1–10 (2008). https://doi.org/10.1038/nprot.2008.23
27 Padmanabha D and Baker KD, Drosophila gains traction as a repurposed tool to investigate metabolism. *Trends Endocrinol Metab* **25**:518–527, Elsevier Ltd (2014).
28 Arrese EL and Soulages JL, Insect fat body: energy, metabolism, and regulation. *Annu Rev Entomol* **55**:207–225 (2010).
29 Li S, Yu X and Feng Q, Fat body biology in the last decade. *Annu Rev Entomol* **64**:315–333 (2019).
30 Bailey AP, Koster G, Guillermier C, Hirst EMA, MacRae JI, Lechene CP *et al*., Antioxidant role for lipid droplets in a stem cell niche of *drosophila*. *Cell* **163**:340–353, The Authors (2015).
31 Feyereisen R, Insect P450 enzymes. *Annu Rev Entomol* **44**:507–533 (1999).
32 Chung H, Sztal T, Pasricha S, Sridhar M, Batterham P and Daborn PJ, Characterization of *Drosophila* melanogaster cytochrome P450 genes. *Proc Natl Acad Sci U S A* **106**:5731–5736 (2009).
33 Harrop TWR, Pearce SL, Daborn PJ and Batterham P, Whole-genome expression analysis in the third instar larval midgut of Drosophila melanogaster. *G3 Genes, Genomes, Genet* **4**:2197–2205 (2014).
34 Enayati AA, Ranson H and Hemingway J, Insect glutathione transferases and insecticide resistance. *Insect Mol Biol* **14**:3–8 (2005).
35 Vontas JG, Small GJ and Hemingway J, Glutathione S-transferases as antioxidant defence agents confer pyrethroid resistance in Nilaparvata lugens. *Biochem J* **357**:65–72 (2001).
36 Darios F and Stevanin G, Impairment of lysosome function and autophagy in rare neurodegenerative diseases. *J Mol Biol* **432**:2714–2734, The Authors (2020).
37 Lakpa KL, Khan N, Afghah Z, Chen X and Geiger JD, Lysosomal stress response (LSR): physiological importance and pathological relevance. *J Neuroimmune Pharmacol* **16**:219–237 (2021).
38 Perry T, Chen W, Ghazali R, Yang YT, Christesen D, Martelli F *et al*., Role of nicotinic acetylcholine receptor subunits in the mode of action of neonicotinoid, sulfoximine and spinosyn insecticides in Drosophila melanogaster. *Insect Biochem Mol Biol* **131**:103547, Elsevier Ltd (2021).
39 Fusetto R, Denecke S, Perry T, O'Hair RAJ and Batterham P, Partitioning the roles of CYP6G1 and gut microbes in the metabolism of the insecticide imidacloprid in Drosophila melanogaster. *Sci Rep* **7**:1–12 (2017).
40 Liu L, Zhang K, Sandoval H, Yamamoto S, Jaiswal M, Sanz E *et al*., Glial lipid droplets and ROS induced by mitochondrial defects promote neurodegeneration. *Cell* **160**:177–190, Elsevier Inc (2015).
41 Liu L, MacKenzie KR, Putluri N, Maletić-Savatić M and Bellen HJ, The glia-neuron lactate shuttle and elevated ROS promote lipid synthesis in neurons and lipid droplet accumulation in glia via APOE/D. *Cell Metab* **26**:719–737.e6 (2017).
42 Freeman MR, *Drosophila* central nervous system glia. *Cold Spring Harb Perspect Biol* **7**:1–14 (2015).
43 Butterworth FM and Bodenstein D, Adipose tissue of Drosophila melanogaster. *Gen Comp Endocrinol* **13**:68–74 (1969).
44 Nelliot A, Bond N and Hoshizaki DK, Fat-body remodeling in Drosophila melanogaster. *genesis* **44**:396–400 (2006).
45 Kogot-Levin A and Saada A, Ceramide and the mitochondrial respiratory chain. *Biochimie* **100**:88–94, Elsevier Masson SAS (2014).
46 Zachman DK, Chicco AJ, McCune SA, Murphy RC, Moore RL and Sparagna GC, The role of calcium-independent phospholipase A2 in cardiolipin remodeling in the spontaneously hypertensive heart failure rat heart. *J Lipid Res* **51**:525–534 (2010).
47 Weber AL, Khan GF, Magwire MM, Tabor CL, Mackay TFC and Anholt RRH, Genome-wide association analysis of oxidative stress resistance in drosophila melanogaster. *PLoS One* **7**:e34745 (2012).
48 Bisht S, Faiq M, Tolahunase M and Dada R, Oxidative stress and male infertility. *Nat Rev Urol* **14**:470–485, Nature Publishing Group (2017).
49 Homem RA, Buttery B, Richardson E, Tan Y, Field LM, Williamson MS *et al*., Evolutionary trade-offs of insecticide resistance — the fitness costs associated with target-site mutations in the nAChR of Drosophila melanogaster. *Mol Ecol* **29**:2661–2675 (2020).
50 Hsu J-C, Feng H-T, Wu W-J, Geib SM, Mao C and Vontas J, Truncated transcripts of nicotinic acetylcholine subunit gene Bdα6 are associated with spinosad resistance in Bactrocera dorsalis. *Insect Biochem Mol Biol* **42**:806–815, Elsevier Ltd (2012).
51 Wang X, Ma Y, Wang F, Yang Y, Wu S and Wu Y, Disruption of nicotinic acetylcholine receptor α6 mediated by CRISPR/Cas9 confers resistance to spinosyns in Plutella xylostella. *Pest Manag Sci* **76**:1618–1625 (2020).
52 Silva WM, Berger M, Bass C, Williamson M, Moura DMN, Ribeiro LMS *et al*., Mutation (G275E) of the nicotinic acetylcholine receptor α6 subunit is associated with high levels of resistance to spinosyns in Tuta absoluta (Meyrick) (Lepidoptera: Gelechiidae). *Pestic Biochem Physiol* **131**:1–8, Elsevier Inc. (2016).
53 Puinean AM, Lansdell SJ, Collins T, Bielza P and Millar NS, A nicotinic acetylcholine receptor transmembrane point mutation (G275E) associated with resistance to spinosad in Frankliniella occidentalis. *J Neurochem* **124**:590–601 (2013).
54 Baxter SW, Chen M, Dawson A, Zhao J-Z, Vogel H, Shelton AM *et al*., Mis-spliced transcripts of nicotinic acetylcholine receptor α6 are associated with Field evolved Spinosad resistance in Plutella xylostella (L.), ed. by stern DL. *PLoS Genet* **6**:e1000802 (2010).
55 Khorram SM, Zhang Q, Lin D, Zheng Y, Fang H and Yu Y, Biochar: a review of its impact on pesticide behavior in soil environments and its potential applications. *J Environ Sci (China)* **44**:269–279, Elsevier B.V. (2016).
56 Müller C, Impacts of sublethal insecticide exposure on insects — facts and knowledge gaps. *Basic Appl Ecol* **30**:1–10, Elsevier GmbH (2018).
57 Karami-Mohajeri S and Abdollahi M, Toxic influence of organophosphate, carbamate, and organochlorine pesticides on cellular metabolism of lipids, proteins, and carbohydrates: a systematic review. *Hum Exp Toxicol* **30**:1119–1140 (2011).
58 Lukaszewicz-Hussain A, Role of oxidative stress in organophosphate insecticide toxicity – short review. *Pestic Biochem Physiol* **98**:145–150, Elsevier Inc (2010).
59 Wang X, Martínez MA, Dai M, Chen D, Ares I, Romero A *et al*., Permethrin-induced oxidative stress and toxicity and metabolism. A review. *Environ Res* **149**:86–104, Elsevier (2016).
60 Wang M, Hu Q, Lv T, Wang Y, Lan Q, Xiang R *et al*., High-resolution 3D spatiotemporal transcriptomic maps of developing drosophila embryos and larvae. *Dev Cell* **57**:1271–1283.e4, The Authors (2022).